Multi-Purpose Drones for Coverage and Transport Applications

Mohammadjavad Khosravi, Saeede Enayati, Hamid Saeedi, Hossein Pishro-Nik

Abstract

Unmanned aerial vehicles (UAVs) have become important in many applications including last-mile deliveries, surveillance and monitoring, and wireless networks. This paper aims to design UAV trajectories that simultaneously perform multiple tasks. We aim to design UAV trajectories that efficiently perform some transportation operation (e.g., package delivery), and at the same time provide uniform coverage over a neighborhood area which is needed for applications such as network coverage, Internet of Things (IoT) devices data collection, wireless power transfer, and surveillance. We first consider multi-task UAVs for a simplified scenario where the neighborhood area is a circular region where UAV missions start from the center and the destinations are assumed to be uniformly distributed on the circle boundary. We propose a trajectory process such that if according to which the UAV's move, a uniform coverage can be achieved while the transport (delivery) efficiency is still preserved. We then consider a more practical scenario in which the transport destinations are arbitrarily distributed in an arbitrarily-shaped region.We show that simultaneous uniform coverage and efficient transport trajectory (e.g. package delivery) is possible for such realistic scenarios. This is shown using both rigorous analysis as well as simulations.

Index Terms

Unmanned aerial vehicles, multi-purpose drones, package delivery, uniform network coverage.

I. Introduction

Commercial unmanned aerial vehicles (UAVs), commonly known as drones, deployed in an unmanned aerial system (UAS), have recently drawn increased interest from private industry and

M. Khosravi, S. Enayati, and H. Pishro-Nik are with the Department of Electrical and Computer Engineering, University of Massachusetts, Amherst, MA,01003 USA, E-mail: mkhosravi@umass.edu, senayati@umas.edu, pishro@engin.umass.edu.

H. Saeedi is with the School of Electrical and Computer Engineering, Tarbiat Modares University, Tehran, Iran, E-mail: hsaeedi@modares.ac.ir

academia, owing to their autonomy, flexibility, and broad range of application domains. With the on-going miniaturization of sensors and processors and ubiquitous wireless connectivity, drones are finding many new uses in enhancing our way of life. Applications of UAV technology exist in agriculture [1], surveying land or infrastructure [2]–[4], cinematography [5] and emergency operations [6]–[8].

An important emerging application of drones is on-demand transport of goods and services. Recently, UAV-based public transport in the form of drone taxi service has been tested [9]. More specifically, package delivery has shown to be cost-competitive relative to traditional ground-based delivery methods [5], [10]–[20]. The drones can provide on-demand, inexpensive, and convenient access to the goods and items already in or near an urban area, including consumer goods, fast-food, medicine, and even on-demand groceries. In the design and scheduling of such transport applications, the goal usually is to minimize the overall transport time/distance [5], [11], [21], [22]. To this end, we can consider the transport (delivery) efficiency as the ratio of the actual distance (time) traveled by the drones to the minimum feasible distance (time) that needs to be traveled to take care of a set of transport jobs. The notion of efficiency will be made precise in Section III.

Another important application of drones is their deployment in communications and surveillance [23]–[43]. In the former case, also mostly referred to as aerial base stations (ABS) [44], UAVs are exploited to provide downlink and uplink communication to the users, data collection from Internet of Things (IoT) devices [45], [46], and transfer wireless power to them [47]–[49]. In many cases, the ABS's are assumed to be moving along some pre-designed trajectories [25], [30], [39]. The latter case, referred to as surveillance drones (SD), is usually associated with the drones that can carry video cameras and transmit video to provide new perspectives in visual surveillance [50]. Although these applications may seem pretty different from the technical viewpoints, they share a common requirement: they usually have to fly along trajectories so as to provide a relatively uniform coverage over the area on which they operate. Throughout this

paper, such applications are referred to as uniform-coverage applications (UCA).

Expectedly in future, several personal and commercial applications of the UAVs will emerge and this causes an exponential increase in the aerial traffic flow [51]. This, consequently, can increase collision probability between the mobile agents. Hence, a potential solution for decreasing the number of simultaneously flying vehicles and hence relieving the air traffic control, is to use them for multiple purposes at the same time. This is in addition to the potential reduction in deploying costs for the operating entity. Therefore, figuring out the principles of designing an efficient multipurpose mechanism for the UAVs is an interesting practical problem.

In this paper, we aim to systematically investigate this idea for the first time. Among different transport applications, we focus on a more mature scenario where in a residential region, drones are used as the last-mile delivery tools within the area. Needless to say, the stated results are easily applicable to any other type of transport application for which the aim is to minimize the overall transport time/distance. Since these drones are already flying all over the area and providing some kind of aerial coverage, we may wish to use them in a UCA framework. If this is the case, an important question would be whether the same mobility patterns can provide a uniform coverage in the area of interest. Alternatively, if we modify the patterns to achieve a uniform coverage, do we necessarily have to lose anything in terms of delivery efficiency?

To get an insight into the proposed question, consider the 780-acre University of Massachusetts (UMASS) campus that contains about 170 buildings (Figure 1a) in which we assume that the last-mile delivery office is located in the lower-left corner of the figure with 10 operating drones. The drones start flying in straight lines with constant velocity to deliver the package to the building of interest and fly back to the post office. It is not difficult to see that this is the most efficient delivery profile[1]. We refer to this fixed-speed direct-line delivery algorithm as the "benchmark algorithm" throughout this paper. Now we investigate the coverage associated to this

[1]It is easy to see that invoking any practical limitation such as safety considerations can only increase the travel distance. Moreover, it is worth noting that the details are not consequential here as the point being made is that normal operation of drones in straight-lines normally creates non-uniform coverage.

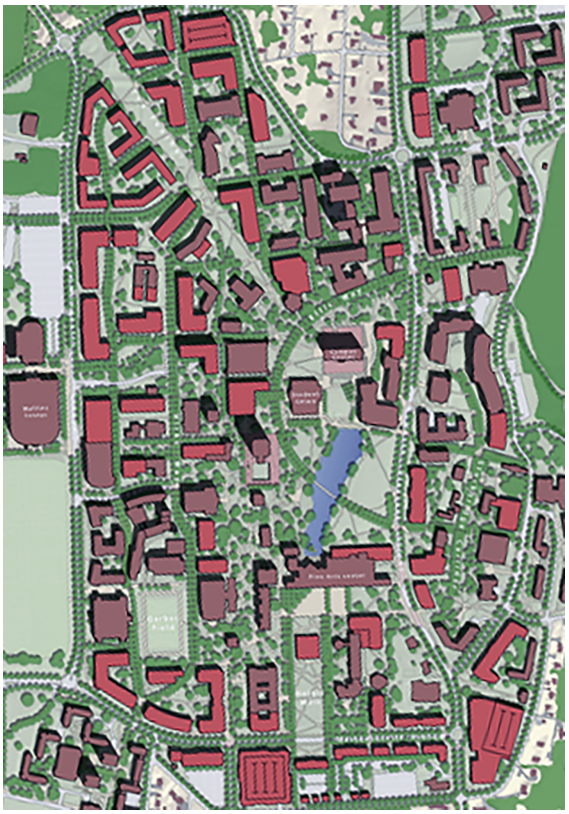

(A) University of Massachusetts (UMASS) campus

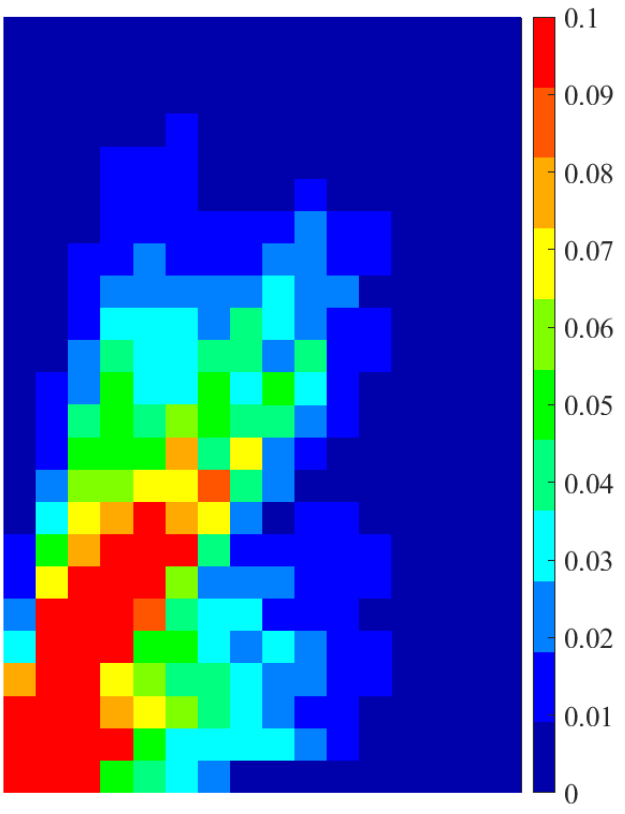

(B) Heat-map of average number of drones for the *fixed-speed-direct-line* algorithm (benchmark)

FIGURE 1: Multi-purpose drone algorithm for a residential area

mobility pattern. To do so, we divide the maps into small regions and find the average number of drones on that region at an arbitrary time instant through a simulation setup. The results have been shown on a heat map in Figure 1b.

As can be seen, the coverage is quite far from uniform which suggests that the idea of multi-purpose UAS may not actually work. Surprisingly, we will demonstrate that this is not the case. In this paper, we design efficient drone delivery systems that can simultaneously provide a fairly uniform coverage. This is achieved through designing mobility trajectories on which the drones move with variable speeds. In this regard, in Section III, we first consider a simplified scenario where we assume a circular region with the post office located at its center (referred to as the ideal case). The houses are assumed to be uniformly distributed on the circle boundary. Assuming the package arrivals are also uniform, we propose a trajectory process such that if

according to which the drones move, a uniform coverage can be achieved while the delivery efficiency tends to 1. After obtaining initial insight on the proposed approach in this scenario, we then consider a practical real-life scenario, namely general case, in Section IV in which the delivery destinations are arbitrarily distributed in an arbitrarily-shaped region. We also do not assume any restrictions on the distribution of arrival packages. In this case, we also show that simultaneous uniform coverage and efficient package delivery is practically possible at the expense of some mild increase in consumed energy. It is worth mentioning that the the novel approach proposed in this scenario, not only is useful to provide a uniform coverage, but also is applicable to any desired pattern of non-uniform coverage across the area.

The rest of the paper is organized as follows: in Section II, we provide some definitions and discussions that are needed throughout the paper. In Section III, we introduce our system model, scenario, our proposed algorithm for the ideal case (simplified scenario) and analytically prove the uniformity of the coverage and the efficiency of package delivery of our proposed algorithm. In Section IV, we present the practical scenario, and after describing the steps of our proposed algorithm, we prove the coverage uniformity. Section V provides the simulation results, and Section VI concludes our work.

II. Preliminaries

A. Binomial Point Processes

If a fixed number of points are independently and identically distributed (i.i.d.) on a compact set $W \in R^d$, we say that these points can be modeled by general binomial point process (BPP) [52]. If these points are distributed uniformly within the same compact set, then we say the points are distributed according to a uniform BPP.

B. Uniform Coverage

We first need to clarify what we exactly mean by a uniform coverage. Uniform coverage can be considered from two perspectives: one is related to ensemble averages, and the other is related to time averages as discussed below. The concept of the former perspective is the same as in [39] where the authors obtain trajectories for UCAs according to the ensemble averages. Specifically,

they aim at designing trajectory processes for which, at any time snapshot, the locations of drones are distributed according to a uniform BPP process over the neighborhood area. This means that for all $t > t_0$, the instantaneous locations of the drones along the delivery path $(\theta_d(t), R_d(t))$, are uniformly distributed over A. Here, the average is taken over any sources of randomness in the scenario.

The other perspective is to look at the time averages. Roughly speaking, if we divide the intended area to small equal cells, we can look at the percentage of the time each cell is covered over time and require that all the cells are covered equally over a long period of time. We will explain this in more rigorous terms in subsection IV-B.

Depending on the application, one of the above definitions might be more useful. Nevertheless, as it turns out, under mild conditions, the trajectory processes can be made ergodic in the sense that both conditions can be satisfied simultaneously [39]. In this paper, we consider the first definition (ensemble average view) for the ideal case in Section III. This is because in that section, we make specific assumptions for probability distributions. On the other hand, in Section IV, since we do not make any specific assumptions about probability distributions, we follow the second definition.

C. Transport Efficiency

Here, we make the notion of transport efficiency precisely. As our focus in this paper is on package delivery, we also refer to this as package delivery efficiency. Let $\mathcal{A}(\mathrm{C})$ be the set of all possible delivery algorithms satisfying the set of conditions and requirements C. For example, for a given geometry, we could require that the algorithms are able to deliver m arriving packages using D drones with the average velocity V_{avg} assuming each drone can carry only one package at a time. Since there is uncertainty and randomness in the operation (for example, the package destinations are not predetermined, and could follow a known or unknown statistical distribution), we need to consider a probabilistic view. More specifically, let the underlying probability space be represented as $(\Omega, \mathcal{F}, P)$, where Ω, $\mathcal{F}$, and P represent the sample space, the event space,

and the probability function, respectively. This probability space captures all non-deterministic aspect of the problem.

Consider an Algorithm $A \in \mathcal{A}(\mathrm{C})$. Let $\mathrm{T}_m(A)$ indicate the expected value of the time to deliver m packages using Algorithm A, where the expectation is taken over the probability space $(\Omega, \mathcal{F}, P)$. Define T_m^* as $T_m^* = \inf\{T_m(A) : A \in \mathcal{A}(\mathrm{C})\}$. Intuitively, T_m^* provides the smallest average delivery time possible in a setting. This gives us a means to define package delivery efficiency for any Algorithm $A \in \mathcal{A}(\mathrm{C})$.

Definition 1. Consider a set of delivery algorithms $\mathcal{A}(\mathrm{C})$ satisfying the set of conditions and requirements C. We define the efficiency of the package delivery for an Algorithm $A \in \mathcal{A}(\mathrm{C})$ as follows

$$\eta = \frac{T_m^*}{T_m(A)}, 0 \leq \eta \leq 1 \tag{1}$$

If η is close to 1, it means that the algorithm is more efficient.

D. Channel Model

Although the work presented in this paper is independent of any channel model assumptions, for the sake of clarity in simulation, we assume that the communication channel between a transmitter-receiver pair undergoes both path-loss and small scale Nakagami-m fading. Therefore, the channel power gain has a Gamma distribution with parameter m as below [27]:

$$f_G(g) = \frac{m^m g^{m-1}}{\Gamma(m)} \exp(-mg). \tag{2}$$

E. Access Delay

The access delay has a strong impact on the experienced quality of communication by the users. In our framework, access delay is caused by non-continuous cell visits by the delivering drones. For a typical cell l, let's denote the delay between the departure of the k^{th} drone and arrival of the $k + 1^{th}$ drone with δ_k. Then, the average access delay time T_{delay} for cell l is the ratio of total access delay time to the total number of visits K during the delivery period for m packages:

$$T_{delay} = \frac{\Sigma_{k=1}^{K} \delta_k}{K}. \tag{3}$$

F. Power consumption

One critical issue of UAV operation is the limited onboard energy of UAVs, which renders energy-efficient UAV communication particularly important. The UAV energy consumption is in general composed of two main components, namely the communication related energy and the propulsion energy. Depending on the size and payload of UAVs, the propulsion power consumption may be much more significant than communication-related power. To this end, proper modeling for UAV propulsion energy consumption is crucial. For a rotary-wing UAV with speed V, the propulsion power consumption can be expressed as [53]:

$$P(v) = P_0(1 + \frac{3v^2}{U_{tip}^2}) + P_i(\sqrt{1 + \frac{v^4}{4v_0^4}} - \frac{v^2}{2v_0^2})^{\frac{1}{2}} + \frac{1}{2}d_0\psi d_A v^3, \tag{4}$$

where P_0 and P_i are constants representing the blade profile power and induced power in hovering status that depends on the aircraft weight, air density ψ, and rotor disc area d_A, as specified in [53], U_{tip} denotes the tip speed of the rotor blade, v_0 is known as the mean rotor induced velocity in hovering, and d_0 and s are the fuselage drag ratio and rotor solidity, respectively.

Therefore, with a given trajectory $q(t)$ where $q(t) \in R^2$ and $0 \leq t \leq T_m$, the propulsion energy consumption can be expressed as

$$E(T_m, q(t)) = \int_0^{T_m} P(||v(t)||)dt, \tag{5}$$

where $||v(t)||$ is the instantaneous UAV speed.

III. Ideal case

Here, we first explain the system model and scenario for the ideal case. Next, we propose our algorithm which delivers the packages and provides the uniform coverage over the region.

A. System model

Figure 2 shows the neighborhood area over which we want to provide the uniform coverage. We assume that D drones deliver the arriving packages from the post office (at the center of region) to the N destination houses and at the same time, they are used for a UCA. There are N houses in the neighborhood area, which are destinations of the arrival packages. The houses are uniformly

and independently distributed at the boundary of the circular region. We assume packages are continuously arriving at the post office center. In other words, it is assumed that there are always packages in the post office to be delivered by the drones. Let $X_1, X_2, X_3, ...$ be the sequence of random variables that correspond to the sequence of incoming packages. More specifically, we say that the i^{th} package must be delivered to the k^{th} house, if $X_i = k$, where $k \in \{1, 2, ..., N\}$.

FIGURE 2: Neighborhood area for Ideal case

To compare efficiency of different algorithms fairly, we assume that all the drones fly with the average velocity, i.e., V_{avg}. The average is computed over the running time of the delivery algorithm. It means that when we compare our algorithm with the benchmark algorithm, the average speed of both algorithms are equal to V_{avg}. The time needed for one drone to reach the neighborhood edge from the post office in a straight line by average velocity V_{avg} is denoted by τ, i.e., $\tau = \frac{\rho - \gamma}{V_{avg}}$ where γ is the radius of the post office center, and ρ is the radius of the entire neighborhood area. Please note that in practice, since the post office radius is very small, its impact is negligible. For simplicity, throughout the paper, we ignore the down times, i.e., nights, and remove them from our analysis.

B. The Scenario for Ideal Case

We assume that D drones deliver the arriving packages from the post office in a circular neighborhood area. Figure 3 shows the parameters of this scenario. θ_i $(0 \leq \theta_i \leq \theta_{max})$ is the angle of the i^{th} house on the perimeter of the circle sector. In case of a full circle, θ_{max} is equal to 2π as in Fig. 2. The whole

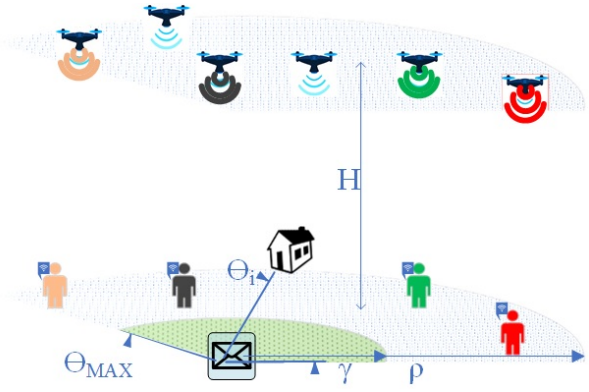

FIGURE 3: Parameters of our system model

neighborhood area A is defined as in (6). We assume houses are distributed uniformly over the neighborhood edge. We also assume package destinations are uniformly distributed over $1, 2, ..., N$.

$$A = \{(r, \theta) : \gamma \leq r \leq \rho; 0 \leq \theta \leq \theta_{max}\} \tag{6}$$

C. Lower bound for T_m^*

Here, we obtain a lower bound for T_m^* for the ideal case.

Lemma 1. In Ideal case, we have $T_m^* \geq \frac{2m\tau}{D}$, where τ and D are defined above.

Proof. Let's first assume there is only one drone. For delivering any of the packages, the drone must travel a distance $d_i \geq 2(\rho - \gamma)$. Note that the equality only happens if the drone follows straight line from the post office to the destination. Let t_i be the time devoted to the delivery of the ith package. Then, the total time for delivery of m packages will be at least $\sum_{i=1}^{m} t_i$ and the total distance traveled is $\sum_{i=1}^{m} d_i$. By assumption, the average speed is V_{avg}, therefore

$$\sum_{i=1}^{m} t_i = \frac{\sum_{i=1}^{m} d_i}{V_{avg}} \geq \frac{2m(\rho - \gamma)}{V_{avg}} = 2m\tau.$$

Now, if there are D drones, for simultaneously delivering m packages, a minimum time of $\frac{2\tau m}{D}$ is necessary. Since this is true for all $A \in \mathcal{A}(\mathrm{C})$, we conclude

$$T_m^* \geq \frac{2m\tau}{D}.$$

□

D. The Algorithm

Here, we propose a multipurpose algorithm for the ideal case, i.e., an algorithm that can be used both for delivery of packages as well as uniform coverage. The simplifying assumptions of the ideal case makes the design of such algorithms very easy for this case. In

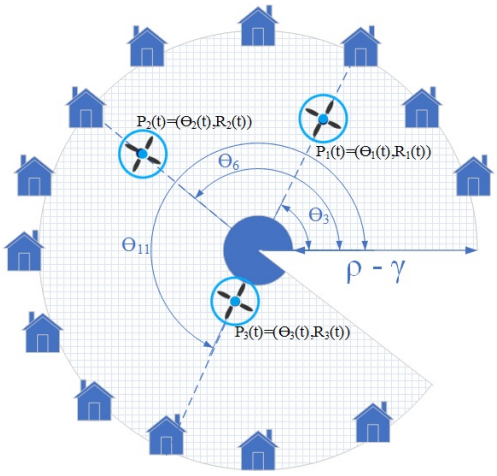

FIGURE 4: First process trajectory

Algorithm 1 Algorithm corresponding to the ideal case

function DELIVERYCOST(D, m, X)

Inputs:

D drones with average speed V

m number of packages to be delivered

X arrival packages which are distributed over $1, 2, ..., N$

Output:

Total time to deliver m packages (T_m)

for <i=1; j<=D> **do**

  Generate random variable T_i uniform over $(0, \tau)$.

  Assign i^{th} package to i^{th} drone

  i^{th} drone flies at T_i over a straight line with $V_d(t)$ at angle θ_i

end for

$j = D + 1$;

while j<=m> **do**

  Assign j^{th} package to a free drone (say i^{th} drone)

  i^{th} drone flies right away over a straight line with $V_d(t)$ at angle θ_j

end while

end function

fact, the main idea comes from properly randomizing the initial take-off times of the drones as well as properly choosing varying speeds for drones during delivery. In the proposed algorithm, referred to as Algorithm 1, first, we choose the take off times of drones, $T_1, T_2, ..., T_D$, independently and uniformly from $(0, \tau)$. A package $X_i = k(1 \leq k \leq N, i = 1, 2, ...)$ is assigned to a free drone to be delivered. Each drone first flies to a predetermined altitude of H, then flies in a straight line with angle θ_k (the direction of the destination) towards the neighborhood edge. When the drone reaches the neighborhood edge and delivers its assigned package, it returns to the origin on the same angle to complete the first cycle and this action repeats continuously. Figure 4 shows this trajectory process.

The speed of drone d at time t is given by

$$V_d(t) = \begin{cases} \frac{(\rho^2-\gamma^2)}{2\sqrt{\tau((\rho^2-\gamma^2)(t-k\tau-T_d)+\tau\gamma^2)}}, & \text{if } T_d + k\tau \leq t \leq T_d + (k+1)\tau, \text{ k even.} \\ \frac{-(\rho^2-\gamma^2)}{2\sqrt{\tau((\rho^2-\gamma^2)((k+1)\tau+T_d-t)+\tau\gamma^2)}}, & \text{if } T_d + k\tau \leq t \leq T_d + (k+1)\tau, \text{ k odd.} \end{cases} \tag{7}$$

We prove that if d^{th} drone flies with speed $V_d(t)$ at time t given by (7), the drones will provide a uniform coverage over the area A. Equation (7) suggests that drones fly faster close to post office and decrease their speed near the boundary (i.e., near the houses) to provide a uniform coverage. Furthermore, the location of the drone is obtained by taking integral of (7) as in (8).

$$R_d(t) = \begin{cases} \sqrt{\frac{(\rho^2-\gamma^2)(t-k\tau-T_d)}{\tau} + \gamma^2}, & \text{if } T_d + k\tau \leq t \leq T_d + (k+1)\tau, \text{ k even.} \\ \sqrt{\frac{(\rho^2-\gamma^2)((k+1)\tau+T_d-t)}{\tau} + \gamma^2}, & \text{if } T_d + k\tau \leq t \leq T_d + (k+1)\tau, \text{ k odd.} \end{cases} \tag{8}$$

Theorem 1. For trajectory process corresponding to the ideal case: i) For all $t > \tau$, the instantaneous locations of the drones along the delivery path $(\theta_d(t), R_d(t))$, form a uniform BPP, and ii) the time to deliver m packages is equal or less than $\frac{2m\tau}{D} + \tau$, i.e., $\mathrm{T}_m(A) \leq \frac{2m\tau}{D} + \tau$.

Before providing the proof, we present the following lemma which will be used later in the proof procedure.

Lemma 2. For any arbitrary observation time of $t > \tau$, the location of any of the D drones that move according to (7) has the following probability density function (pdf):

$$f_{R_d}(r_d) = \frac{2r_d}{\rho^2 - \gamma^2}, \quad \gamma \leq r_d \leq \rho.$$

That is, $f_{R_d}(r_d)$ is the pdf of distance of a uniformly distributed point in the circular region between radii γ and ρ.

Proof. First, assume that $T_d + k\tau \leq t \leq T_d + (k+1)\tau$ and k is odd, we have the following:

$$\begin{aligned} F_{R_d}(r_d) &= Pr(R_d(t) \leq r_d) = Pr(\sqrt{\frac{(\rho^2-\gamma^2)((k+1)\tau+T_d-t)}{\tau} + \gamma^2} \leq r_d) \\ &= Pr(T_d \leq \frac{\tau(r_d^2-\gamma^2)}{\rho^2-\gamma^2} - (k+1)\tau + t) = Pr(T_d \leq \omega_d) = F_{T_d}(\omega_d), \end{aligned} \tag{9}$$

where F_{T_d} is the CDF of T_d and $\omega_d = \frac{\tau(r_d^2-\gamma^2)}{\rho^2-\gamma^2} - (k+1)\tau + t$.

Now to obtain the PDF of the R_d, we take the derivative of F_{R_d}:

$$f_{R_d}(r_d) = \frac{dF_{R_d}(r_d)}{dr_d} = \frac{dF_{T_d}(\omega_d)}{dr_d} = \frac{d}{dr_d}(\frac{r_d^2-\gamma^2}{\rho^2-\gamma^2} - (k+1) + \frac{t}{\tau}) = \frac{2r_d}{\rho^2-\gamma^2}, \quad \gamma \leq r_d \leq \rho \tag{10}$$

where (10) is obtained from the fact that $T_d \sim U(0,\tau)$. The case for even k is proved similarly. □

We now provide the proof for Theorem 1.

Proof. To prove the first part of Theorem 1, we first need to show that for $t > \tau$, the location of vehicles are independent. This is intuitive, since $\theta_d \sim U(0,\theta_{max})$ and $T_d \sim U(0,\tau)$ both have been chosen independently. Second, we have to show that the locations are uniformly distributed over A. To do so, we note that since, $\theta_d \sim U(0,\theta_{max})$, the angle of the drone is uniformly distributed between 0 and θ_{max}, i.e. $\angle P_d(t) \sim U(0,\theta_{max})$. In addition, in Lemma 2, we proved that the location of drones, i.e., $R_d(t)$, are uniformly distributed over A. Therefore, drones are distributed according to uniform BPP over A.

The proof of the second part of Theorem 1 is as follows: The departure times of the D drones, $T_1, T_2, ..., T_D$, are i.i.d. and uniform over $(0,\tau)$. So by time τ, all D drones have departed and by time 3τ, they have delivered at least D packages and come back to the post office center. The delivery time of the rest of packages (i.e., $m-D$ packages) is $\frac{2\tau(m-D)}{D}$, which are simultaneously delivered by the D drones. Therefore, the time to deliver m packages is equal to or less than $\frac{2m\tau}{D} + \tau$. □

By considering the upper bound of $T_m(A)$ obtained in Theorem 1, and the lower bound of delivery efficiency time obtained in Lemma 1, the efficiency of the proposed algorithm satisfies

$$\eta \geq \frac{1}{1+\frac{D}{2m}}. \tag{11}$$

Note that since m is the number of delivered packages, the efficiency approaches 1 over time.

IV. PRACTICAL (GENERAL) CASE

In the general scenario, we avoid imposing any specific assumptions on the density and location of homes, or the distribution of arrival packages. Instead, we consider an area with arbitrarily given geometry and its corresponding parameters. Hence, this setting can be applied to any neighborhood area.

A. System Model and the Scenario

FIGURE 5: Neighborhood areas for Practical case

Figure 5 shows a typical neighborhood area over which we aim to provide a uniform coverage. In this case, the geometry of neighborhood area does not need to be circular and is generally represented by a 2D shape. In addition, the houses are arbitrarily distributed in the neighborhood area, so the distances from the post office to the houses can be any arbitrary value. Again, we consider a multipurpose scenario: We assume that D drones deliver the arriving packages from the post office to N destination houses and at the same time, we aim to use them in a UCA framework. We assume packages are continuously arriving at the post office center. The only assumption we make (about the probability distributions of the destinations) is that over a period of time, each destination has non-zero probability. The location of h^{th} house is defined in a three-dimensional (3D) Cartesian coordinate system by $(x_h, y_h, 0)$, where $1 \leq h \leq N$. Drones fly at a constant altitude H above the ground and the location of the d^{th} drone at time t is shown by $(X_d(t), Y_d(t), H)$, where $1 \leq d \leq D$.

B. The Algorithm

Here, we provide the detailed steps and components of the algorithm for the practical case. **Division of the area to small equal cells:** In this algorithm, referred to as Algorithm 2, first, we divide the neighborhood area into small equal regions (cells). We use A_l to refer to these regions where $1 \leq l \leq S$ and S is the number of cells. We assume that A_l is small so that at

most one drone can fly over the cell at any time. This assumption is compatible with the safety concern of drones as well. It should be noted that the algorithm can be easily extended to the case where we divide the area to the non-equal cells.

Defining Trajectories: Then, we should define the trajectory paths, $PT_h : 1 \leq h \leq N$, between the post office and the houses in order to deliver the packages with high efficiency and simultaneously provide the uniform coverage. If we were not concerned about the UCA requirement, the most efficient trajectories would have been straight lines from post office to the destinations. Nevertheless, to achieve the UCA requirement, we might need to change trajectories slightly: If needed, we change the straight lines between the post office and the houses in a way that all defined small regions are crossed by at least one trajectory. It means that we need to make sure $((\cup_{h=1}^{N} PT_h) \cap A_l \neq \varnothing)$ for any region l, $1 \leq l \leq S$.

Uniform Coverage: Here, we specifically state the requirement for uniform coverage. Consider the time interval $[0, t]$ where packages are continuously being delivered to their destinations. For any cell l, define $c_l(t)$ as the total time that cell is covered (i.e., a drone is flying over that region). The coverage ratio up to time t is defined as $p_l(t) = \frac{c_l(t)}{t}$. For uniform coverage, we require that for all cells $l = 1, 2, \cdots, S$, we must have $\lim_{t\to\infty} p_l(t) = p^*$, where p^* is the desired coverage probability. It is worth noting that although to have a rigorous proof we state the condition for the limit case, in practice the convergence is fast as observed in our simulations in Section V.

Varying Drone Speeds: Algorithm 2 is an *adaptive* algorithm, that is, we adjust the velocity of drones when they enter the regions in order to preserve the uniformity in all cells. Intuitively, if the current coverage ratio is less than the desired coverage probability p^* (i.e., $p_l(t) < p^*$), we should decrease the velocity of the drone, and if it is more than the expected coverage probability, the drone should pass this region faster. Lines 21 to 25 of Algorithm 2 show this adjustment, where H_1 is Hausdorff measure.

In what follows, we show that we can adjust the velocities in a way to guarantee $\lim_{t\to\infty} p_l(t) = p^*$ for all cells, A_l, $l = 1, 2, \cdots, S$. For notational simplicity, we will sometimes drop the subscript

Algorithm 2 Algorithm corresponding to the practical case

function DELIVERYCOST(A, D, m, X)

Inputs:

A the area should be covered

D drones with average speed V

m number-of packages to deliver

X arrival packages which are not uniformly distributed over $1, 2, ..., N$

Output:

Total time to deliver m packages (T_m)

Define V_{MAX} and V_{MIN}

Divide A into small equal cells; called these cells $A_1, A_2, ..., A_S$

for each small cells consider coverage probability p_l , $1 < l < S$ and initialize it with 0

for *h=1;* $h <= N$ **do**

Generate the straight trajectory between the post office and h^{th} house and called it PT_h

end for

for *l=1;* $l <= S$ **do**

if No PT passes through A_l **then**

Select PT_h which is the closest trajectory to A_l

Change PT_h in such a way that it passes through A_l

end if

end for

for *j=1;* $j <= \frac{m}{D}$ **do**

for *i=1;* $i <= D$ **do**

Assign $((j-1) * D + i)^{th}$ package to i^{th} drone

Assume h is the destination of $((j-1) * D + i)^{th}$ package

foreach region l which PT_h passes through

if $p_l < p^*$ **then**

Set velocity of i^{th} drone to $MAX(V_{MIN}, \frac{H_1(PT_h, A_l)}{p^* - p_l}(1 - p^*))$

else

Set velocity of i^{th} drone to V_{MAX}

end if

Update p_l

end for

end for

end function

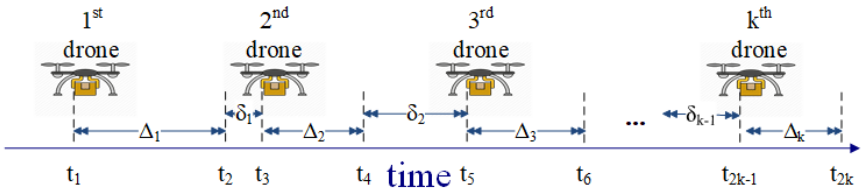

FIGURE 6: Arrival/depature of drones over time within a cell

l in the rest of the proof. Define L as $H_1((\cup_{h=1}^{N} PT_h) \cap A_l)$, i.e., the lengths of the part of trajectories restricted to cell l. Fig. 6 demonstrates arrival/departure of drones over the region during a delivery period for m packages. As you can see, first the drone arrives over the region at time t_1 and traverses the cell with speed V_1, and leaves the region at time t_2. In general, the k^{th} drone arrives over the cell at time t_{2k-1} and leaves the region at time t_{2k} (traverses the cell with speed V_k). The time between the arrival and departure of the k^{th} drone in cell l is denoted by Δ_k and the time between departure of the k^{th} drone and arrival of the $(k+1)^{th}$ is shown by δ_k. Thus,

$$\Delta_k = t_{2k} - t_{2k-1}, \text{and } \delta_k = t_{2k+1} - t_{2k}.$$

Suppose the maximum and minimum possible speeds of drones are given by V_{MAX} and V_{MIN}. If we define $\Delta_{MAX} = \frac{L}{V_{MIN}}$ and $\Delta_{MIN} = \frac{L}{V_{MAX}}$, then we have $0 < \Delta_{MIN} \leq \Delta_k \leq \Delta_{MAX}$. In any practical scenarios, the δ_k values can not be unlimited. So here we assume that there exist $\delta_{MIN} \geq 0$ and $\delta_{MAX} \geq 0$ such that for all k, $0 < \delta_{MIN} \leq \delta_k \leq \delta_{MAX}$. Before stating and proving the main theorem, we need the following definition:

Definition 2. (Causal Velocity Profiles) An algorithm for determining V_j for $j = 1, 2, \ldots$ is said to be casual, if the value of V_j is determined only by the past data up-to time t_{2j-1}.

Theorem 2. If V_{MIN} and V_{MAX} can be chosen such that $V_{MAX} \geq \frac{L(1-p^*)}{p^* \delta_{MIN}}$ and $V_{MIN} \leq \frac{L(1-p^*)}{p^* \delta_{MAX}}$,

then there exists a causal velocity profile such that $\lim_{t\to\infty} p_l(t) = p^*$.[2]

Before proving this theorem, we provide some lemmas that are later used during the proof. Also for simplicity, we assume that only one path goes through A_l (The proof can easily be extended to multiple paths). Since at any time, at most one drone flies over each cell, we can say that $c_l(t_{2k}) = \Sigma_{i=1}^{k}\Delta_k$ and also $c_l(t_{2k+1}) = \Sigma_{i=1}^{k}\Delta_i$. From these statements, the following equations can be concluded:

$$p(t_{2k}) = \frac{c(t_{2k})}{t_{2k}} = \frac{\Sigma_{i=1}^{k}\Delta_i}{t_1 + \Sigma_{i=1}^{k}\Delta_i + \Sigma_{i=1}^{k-1}\delta_j}. \tag{12}$$

$$p(t_{2k+1}) = \frac{c(t_{2k+1})}{t_{2k+1}} = \frac{\Sigma_{i=1}^{k}\Delta_i}{t_1 + \Sigma_{i=1}^{k}(\Delta_i + \delta_i)}. \tag{13}$$

Lemma 3. If all drones traverse the cell with maximum speed at any time i.e. $V_j = V_{MAX}$ for all j, then $\limsup_{k\to\infty} p(t_{2k}) \leq p^*$ and if all drones traverse the cell with minimum speed at any time i.e. $V_j = V_{MIN}$ for all j, then $\liminf_{k\to\infty} p(t_{2k+1}) \geq p^*$.

Proof of Lemma 3. If all drones pass the cell with the maximum velocity V_{MAX}, it takes $\frac{L}{V_{MAX}}$ to leave the cell and we can obtain the probability coverage as follows:

$$P(t_{2k+1}) = \frac{\Sigma_{i=1}^{k}\Delta_i}{t_1 + \Sigma_{i=1}^{k}\Delta_i + \Sigma_{i=1}^{k}\delta_j} = \frac{\frac{kL}{V_{MAX}}}{t_1 + \frac{kL}{V_{MAX}} + \Sigma_{i=1}^{k}\delta_j} = \frac{1}{1 + \frac{t_1 V_{MAX}}{kL} + \frac{V_{MAX}}{kL}\Sigma_{i=1}^{k}\delta_j}.$$

By using $V_{MAX} \geq \frac{L(1-p^*)}{p^*\delta_{MIN}}$, we have

$$\frac{1}{1 + \frac{t_1 V_{MAX}}{kL} + \frac{V_{MAX}}{kL}\Sigma_{i=1}^{k}\delta_j} \leq \frac{1}{1 + \frac{t_1 V_{MAX}}{kL} + \frac{1-p^*}{p^*\delta_{MIN}}(\frac{1}{k}\Sigma_{i=1}^{k}\delta_j)},$$

and since $(\frac{1}{k}\Sigma_{i=1}^{k}\delta_j) \geq \delta_{MIN}$, we have

$$\limsup_{k\to\infty} p(t_{2k+1}) \leq \frac{1}{1 + \frac{1-p^*}{p^*}1},$$

[2]This theorem is a main result stating that the UCA requirement can be satisfied. The conditions V_{MIN} and V_{MAX} simply state that we should be able to have a large enough range for the velocities to be able to achieve a uniform coverage. The proof is given below, which is a bit technical due to the fact that we want to prove the statement in a very general scenario without making specific assumptions. The readers less interested in the technical proof, can refer to Section V to see the simulation results showing the performance of the proposed algorithms for two real neighborhood areas: University of Massachusetts Amherst and Union Point, which is a smart city near Boston.

and as a result, $\limsup_{k\to\infty} p(t_{2k+1}) \leq p^*$.

Next, we show that if all drones traverse the cell with minimum speed at any time i.e., $V_j = V_{MIN}$ for all j, then $\liminf_{k\to\infty} p(t_{2k+1}) \geq p^*$. In this case,

$$P(t_{2k+1}) = \frac{\Sigma_{i=1}^{k}\Delta_i}{t_1 + \Sigma_{i=1}^{k}\Delta_i + \Sigma_{i=1}^{k}\delta_j} = \frac{\frac{kL}{V_{MIN}}}{t_1 + \frac{kL}{V_{MIN}} + \Sigma_{i=1}^{k}\delta_j} = \frac{1}{1 + \frac{t_1 V_{MIN}}{kL} + \frac{V_{MIN}}{kL}\Sigma_{i=1}^{k}\delta_j}.$$

By using $V_{MIN} \leq \frac{L(1-p^*)}{p^*\delta_{MAX}}$, we have

$$\frac{1}{1 + \frac{t_1 V_{MIN}}{kL} + \frac{V_{MIN}}{kL}\Sigma_{i=1}^{k}\delta_j} \geq \frac{1}{1 + \frac{t_1 V_{MIN}}{kL} + \frac{1-p^*}{p^*\delta_{MAX}}(\frac{1}{k}\Sigma_{i=1}^{k}\delta_j)} = \frac{1}{1 + \frac{t_1 V_{MIN}}{kL} + \frac{1-p^*}{p^*}(\frac{1}{k\delta_{MAX}}\Sigma_{i=1}^{k-1}\delta_j)},$$

and since $(\frac{1}{k}\Sigma_{i=1}^{k}\delta_j) \leq \delta_{MAX}$, we have

$$\liminf_{k\to\infty} p(t_{2k+1}) \geq \frac{1}{1 + \frac{1-p^*}{p^*}1},$$

as a result of which, $\liminf_{k\to\infty} p(t_{2k+1}) \geq p^*$. □

Note that the above argument can be repeated for the cases where the first k_0 values of V_j's are arbitrary as they do not impact the limiting behavior. Hence, we provide the following corollary.

Corollary 1. Let k_0 be a positive integer. If we have a sequence V_j for $j = 1, 2, \ldots, \infty$ such that for all $j \geq k_0$, $V_j = V_{MAX}$, then

$$\limsup_{k\to\infty} p(t_{2k+1}) \leq p^*. \tag{A}$$

Similarly, If we have a sequence V_j for $j = 1, 2, \ldots, \infty$ such that for all $j \geq k_0$, $V_j = V_{MIN}$, then

$$\liminf_{k\to\infty} p(t_{2k+1}) \geq p^*. \tag{B}$$

For the brevity of the notation, let's define $p(t_{2k+1}, V_{MIN})$ as the value of $p(t_{2k+1})$ when for all $j \geq k_0$, $V_j = V_{MIN}$, and define $p(t_{2k+1}, V_{MAX})$, similarly. Thus, we have

$$\liminf_{k\to\infty} p(t_{2k+1}, V_{MIN}) \geq p^*.$$

Now consider two cases: If we have

$$\limsup_{k\to\infty} p(t_{2k+1}, V_{MIN}) \leq p^*,$$

then, we will have

$$\lim_{k\to\infty} p(t_{2k+1}, V_{MIN}) = p^*.$$

Otherwise, we must have

$$\limsup_{k\to\infty} p(t_{2k+1}, V_{MIN}) > p^*.$$

So we come up with the following corollaries:

Corollary 2. For any sequence of $p(t_{2k+1})$, one of the following is true:

$$\lim_{k\to\infty} p(t_{2k+1}, V_{MIN}) = p^*, \text{or } \limsup_{k\to\infty} p(t_{2k+1}, V_{MIN}) > p^*.$$

Corollary 3. For any sequence of $p(t_{2k+1})$, one of the following is true:

$$\lim_{k\to\infty} p(t_{2k+1}, V_{MAX}) = p^*, \text{ or } \liminf_{k\to\infty} p(t_{2k+1}, V_{MAX}) < p^*.$$

Definition 3. (Min-Max Algorithm) The min-max algorithm for choosing V_i's is defined as follows: We choose $V_1 = V_{MIN}$. For $k \geq 1$, if $p(t_{2k-1}) \leq p^*$, then $V_k = V_{MIN}$, otherwise $V_k = V_{MAX}$.

Note: The min-max algorithm is used below to prove Theorem 2. Nevertheless, there are various choices of velocity profiles $V_j, j = 1, 2, \ldots, \infty$ that satisfy Theorem 2. Their differences are in their rate of convergence and their practicality. The one we have chosen in our algorithm provides a very fast convergence (Algorithm 2) and also results in much smoother operation (the changes in speeds can actually be made minimal and gradual suitable for practical implementation). However, for the sake of proofs, it is easier to use the min-max algorithm defined above.

Lemma 4. For the min-max algorithm, the following statements are true:

1) If $p(t_{2k-1}) < p^*$, then $p(t_{2k+1}) \geq p(t_{2k-1})$.
2) If $p(t_{2k-1}) > p^*$, then $p(t_{2k+1}) \leq p(t_{2k-1})$.

Proof. If $p(t_{2k-1}) < p^*$, then $V_k = V_{MIN}$, so $\Delta_k = \Delta_{MAX} = \frac{L}{V_{MIN}}$.

$$p(t_{2k+1}) = \frac{c(t_{2k+1})}{t_{2k+1}} = \frac{c(t_{2k-1}) + \Delta_{MAX}}{t_{2k-1} + \Delta_{MAX} + \delta_k} \tag{10}$$

Now note that

$$\frac{\Delta_{MAX}}{\Delta_{MAX} + \delta_k} \geq \frac{\Delta_{MAX}}{\Delta_{MAX} + \delta_{MAX}} \geq p^*. \tag{11}$$

The last inequality is the direct result of the main assumption $V_{MIN} \leq \frac{L(1-p^*)}{p^*\delta_{MAX}}$. Now by combining $p(t_{2k-1}) = \frac{c(t_{2k-1})}{t_{2k-1}} < p^*$ and Equations 10 and 11, we conclude $p(t_{2k+1}) \geq p(t_{2k-1})$. The second statement of the lemma can be proved similarly. □

Lemma 5. For the min-max algorithm, we have $\lim_{j\to\infty} |p(t_{j+1}) - p(t_j)| = 0$.

Proof. It suffices to show $\lim_{k\to\infty} |p(t_{2k}) - p(t_{2k+1})| = 0$ and $\lim_{k\to\infty} |p(t_{2k}) - p(t_{2k-1})| = 0$. The proofs are similar, so we just show the first one. Recall that $P(t_{2k}) = \frac{\Sigma_{i=1}^{k}\Delta_i}{t_1+\Sigma_{i=1}^{k}\Delta_i+\Sigma_{j=1}^{k-1}\delta_j} = \frac{U_k}{W_k}$. Thus, we have $p(t_{2k+1}) = \frac{U_k}{W_k+\delta_k}$. Remember, that for $\delta_{MIN} \geq 0$ and $\delta_{MAX} \geq 0$, we have, $0 < \delta_{MIN} \leq \delta_k \leq \delta_{MAX}$ and $0 < \Delta_{MIN} \leq \Delta_k \leq \Delta_{MAX}$, $\forall k$. We have

$$\begin{cases} k\Delta_{MIN} \leq U_k \leq k\Delta_{MAX} \\ t_1 + k\Delta_{MIN} + (k-1)\delta_{MIN} \leq W_k \leq t_1 + k\Delta_{MAX} + (k-1)\delta_{MAX} \end{cases}.$$

Thus, $\lim_{k\to\infty} U_k = \infty$ and $\lim_{k\to\infty} W_k = \infty$, and their ratio $\frac{W_k}{U_k}$ is bounded. Therefore, we can conclude that

$$\left|p(t_{2k}) - p(t_{2(k+1)})\right| = \frac{\delta_k U_k}{(W_k+\delta_k)(W_k)} \to 0$$

as k goes to infinity. □

Lemma 6. There exists a casual algorithm V_j for $j = 1, 2, \ldots, \infty$ such that

$$\lim_{j\to\infty} p(t_j) = p^*. \tag{12}$$

Proof. Based on Lemma 5, it suffices to show $\lim_{k\to\infty} p(t_{2k+1}) = p^*$. We claim that using the min-max velocity profile, we can achieve $\lim_{k\to\infty} p(t_{2k+1}) = p^*$. Let $p(t_3) \leq p^*$, then the min-max algorithm adjusts V_2 to V_{MIN}. In fact, V_{j+1} is tuned to V_{MIN} as long as $p(t_{2j+1}) \leq p^*$. Now, if for all $j > 1$, $p(t_{2j+1}, V_{MIN}) \leq p^*$ then by Corollary 2, we have $\lim_{k\to\infty} p(t_{2k+1}, V_{MIN}) = p^*$, in which case we are done. Otherwise, there exists a k_1 in which $p(t_{2k_1+1}) \geq p^*$ at which point the algorithm switches to V_{MAX}. Similarly, by Corollary 3, there exists $k_2 \geq k_1$ such that $p(t_{2k_2+1}) \leq p^*$, and this oscillation repeats infinitely (or anytime it stops we are already

converging to p^* and we are done). Thus, we may assume the sequence $p(t_j)$, for $j = 1, 2, \ldots$ **crosses** p^* infinitely many times.

To complete the proof of Lemma 6, we show that for all $\epsilon > 0$, there exists k_ϵ such that for all $k > k_\epsilon$, we have $|p(t_{2k+1}) - p^*| < \epsilon$. First, choose k_1 such that for all $k \geq k_1$, we have $\left|p(t_{2k}) - p(t_{2(k-1)})\right| < \frac{\epsilon}{4}$ and $|p(t_{2k+1}) - p(t_{2k-1})| < \frac{\epsilon}{4}$ (Lemma 5).

Without loss of generality assume $p(t_{2k-1}) < p^*$. Let k_ϵ be the smallest $k > k_1$ such that $p(t_{2k_\epsilon+1})$ crosses p^*, then we know the following

1) $p(t_{2k_\epsilon+1}) > p^*$ and $p(t_{2k_\epsilon+3}) < p(t_{2k_\epsilon+1})$ (Lemma 4);

2) $|p(t_{2k_\epsilon+1}) - p^*| < \frac{\epsilon}{2}$;

3) $|p(t_{2k_\epsilon+3}) - p(t_{2k_\epsilon+1})| < \frac{\epsilon}{2}$.

Therefore, we conclude $|p(t_{2k_\epsilon+3}) - p^*| < \epsilon$. Indeed, repeating the same argument from now on, we conclude that for all $k > k_\epsilon$, we have $|p(t_{2k+1}) - p^*| < \epsilon$. □

Proof of Theorem 2. To prove Theorem 2, we show that the min-max sequence V_j satisfies $\lim_{t\to\infty} p_l(t) = p^*$. It should be noted that we assumed that there exist $\delta_{MIN} > 0$ and $\delta_{MAX} > 0$ such that for all k, $0 < \delta_{MIN} \leq \delta_k \leq \delta_{MAX} < \infty$, also there are $\Delta_{MIN} > 0$ and $\Delta_{MAX} > 0$ such that for all k, $0 < \Delta_{MIN} \leq \Delta_k \leq \Delta_{MAX} < \infty$.

Here, we define $k(t) = min\,(k : t_{2k} \geq t)$. Also, for $t_{2(k-1)} \leq t \leq t_{2k}$ we define the following:

$$a_k = \frac{c(t_{2k})}{t_{2k} - \delta_{MAX} - \Delta_{MAX}},\ b_k = \frac{c(t_{2(k-1)})}{t_{2(k-1)} + \delta_{MAX} + \Delta_{MAX}}.$$

By using (12), we have

$$\lim_{k\to\infty} a_k = \lim_{k\to\infty} \frac{c(t_{2k})}{t_{2k} - \delta_{MAX} - \Delta_{MAX}} = \lim_{k\to\infty} \frac{c(t_{2k})}{t_{2k}} \frac{t_{2k}}{t_{2k} - \delta_{MAX} - \Delta_{MAX}} = p^*.$$

Similarly, we can conclude that

$$\lim_{k\to\infty} b_k = \lim_{k\to\infty} \frac{c(t_{2(k-1)})}{t_{2(k-1)} + \delta_{MAX} + \Delta_{MAX}} = \lim_{k\to\infty} \frac{c(t_{2(k-1)})}{t_{2(k-1)}} \frac{t_{2(k-1)}}{t_{2(k-1)} + \delta_{MAX} + \Delta_{MAX}} = p^*.$$

Using definition of $k(t)$, we have

$$p(t) = \frac{c(t)}{t} \leq \frac{c(t_{2k})}{t} \leq \frac{c(t_{2k}))}{t - \delta_{MAX} - \Delta_{MAX}} = a_k$$
$$.p(t) = \frac{c(t)}{t} \geq \frac{c(t_{2(k-1)})}{t} \geq \frac{c(t_{2(k-1)}))}{t + \delta_{MAX} + \Delta_{MAX}} = b_k.$$

Therefore, for all t, we have $b_k(t) \leq p(t) \leq a_k(t)$. Based on this we can conclude that:

$$\begin{cases} p(t) \geq b_k(t) \\ p(t) \leq a_k(t) \end{cases} \Rightarrow \begin{cases} \liminf\limits_{t\to\infty} p(t) \geq \liminf\limits_{t\to\infty} b_k(t) = p^* \\ \limsup\limits_{t\to\infty} p(t) \leq \limsup\limits_{t\to\infty} a_k(t) = p^* \end{cases} \Rightarrow \lim_{t\to\infty} p(t) = p^*.$$

□

V. Simulation Results

A. Coverage Uniformity Assessment

In Section III, we proved that the ideal algorithm provides uniform coverage, in this section, we run simulation for this algorithm to verify our claim. As mentioned before, to investigate the coverage associated to each trajectory, we divide the neighborhood area into small cells and measure the average number of drones over the regions through simulation. We consider 10 disjoint equal cells within $\frac{5}{8}$ of a circular area with radius $\rho = 5$km as shown in Fig. 7. We set the radius of the post office center to 100, i.e., $\gamma = 100$m, and the number of houses to 100, i.e., $N = 100$. We run the simulation with two different number of drones $D = 5$ and $D = 10$.

Figure 8 shows the average number of drones flying over each of the ten regions for proposed and benchmark algorithms. As can be seen, there are an equal number of drones over all the regions for the proposed algorithm for both 5 and 10 drones, therefore our proposed algorithm provides a uniform coverage. However, the benchmark algorithm has provided a non-uniform coverage.

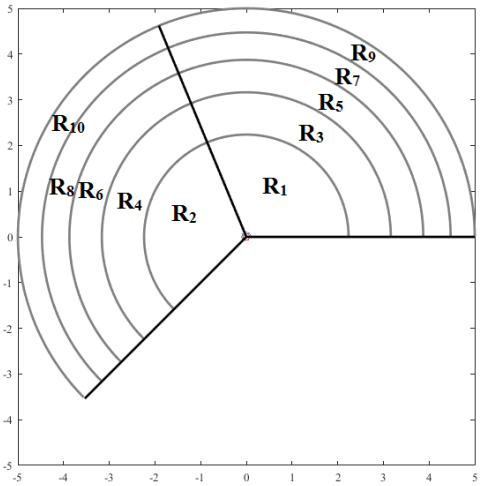

Figure 7: Circular area with radius 5 km is divided to 10 disjoint regions

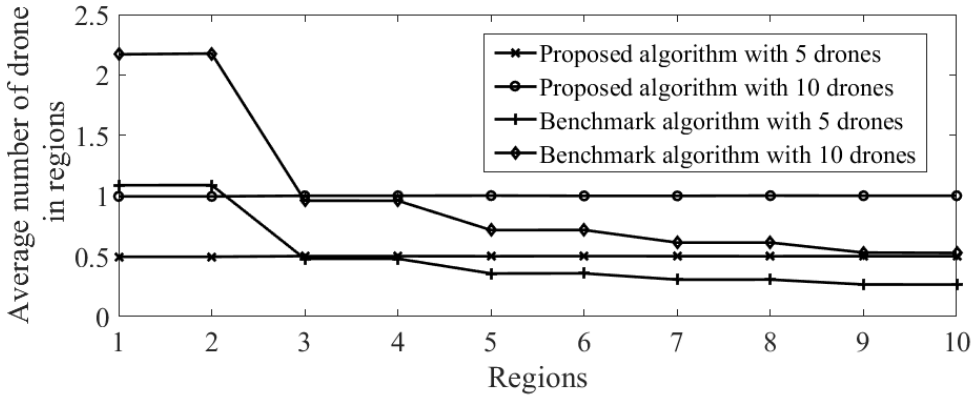

FIGURE 8: Average number of the drones over the regions for 5 and 10 drones

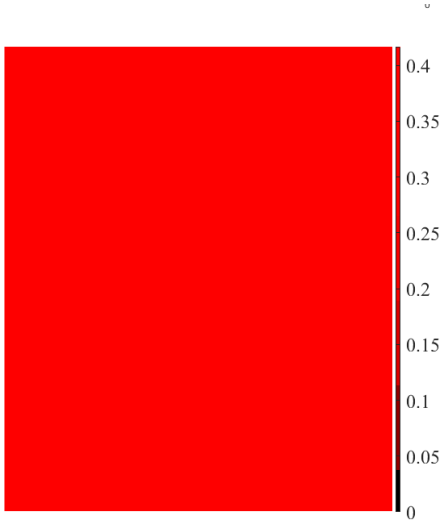

FIGURE 9: Proposed multi-purpose drone algorithm for University of Massachusetts (UMASS) community

In Section IV, we proposed Algorithm 2 to deliver the packages and provide a uniform coverage simultaneously which can be applied to any neighborhood area with any distribution of arrival packages and position of houses. We consider two neighborhood areas, University of Massachusetts Amherst and Union Point, which is a smart town near Boston, to verify our claim about uniformity in coverage and investigate the efficiency of our algorithm to deliver the packages. We introduced University of Massachusetts Amherst community in Section I. Figure 1a and 1b showed the neighborhood map and the heat-map of average number of drones for the benchmark algorithm, respectively. Figure 9 shows the heat-map of the average number of drones for the proposed algorithm. In this figure, our algorithm is simulated with 10 drones. As can be seen, the proposed algorithm has been able to provide uniform coverage over the neighborhood area in contrast to the benchmark algorithm.

As for the Union Point, which has approximately 4000 homes [54] and a total area of 1500 acres (see Fig. 10a), we assume that the last-mile delivery office is located in the top-left corner

of the figure. We divided the neighborhood community into 24 small cells to investigate the coverage. 10 drones are used to deliver the packages.

First, we assume that the drones fly in straight lines with constant velocity to deliver the packages to the houses. The average number of drones flown over the regions is shown by a heat-map in Fig. 10b. Then we assume that the drones follow the proposed Algorithm 2 to deliver the packages to houses. The average number of drones over the regions is shown by heat-map in Fig. 10c. As can be seen, the proposed algorithm provides uniform coverage over the entire neighborhood area.

So far, we only considered average number of drones per unit area to measure the coverage uniformity. Now assume that we are dealing with a specific application such as IoT sensors data collection which includes an uplink wireless communication. In this regard, we define the coverage probability as the probability that the received power by the UAV is above a certain threshold β. We assumed the transmit power of a typical sensor to be 0dBm and considered Nakagami-fading with $m = 2$. We set the Signal to Interference Ratio (SIR) threshold β to be -10 dB. In Fig. 11, we obtained the coverage probability corresponding to the proposed algorithm for both UMASS campus and Union Point community. As can be seen, the coverage probability over both regions is almost uniform.

Now let's see the expected time in which a typical user in the area should wait to have channel access, i.e., average access delay T_{delay}. Through our simulations, we have obtained T_{delay} when delivering $m = 1000$ packages (we obtain T_{dealy} for each cell and average over all cells). This has been done for both the benchmark and the proposed algorithm over both UMASS and Union Point communities and the result is reported in Table I. As can be seen, the average access delay of a typical user in Union Point area is very high (infinity) for the benchmark algorithm because some cells are not covered at all during package delivery. Moreover, the average access delay is less for the UMASS community compared to the Union Point community.

TABLE I: Average access delay time (second) during a delivery period of 1000 packages

	Benchmark algorithm	Proposed algorithm
UMASS community	31.68	16.06
Union Point community	Inf	19.12

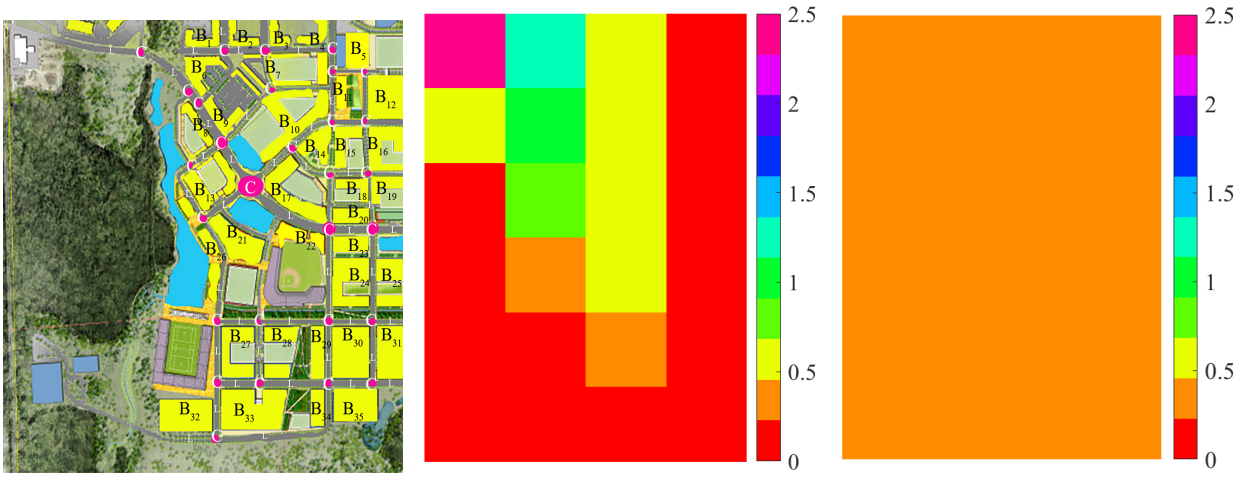

(A) Union Point

(B) Heat-map of average number of drones for the *fixed-speed-direct-line (benchmark)* algorithm

(C) Heat-map of average number of drones for the *proposed* algorithm

FIGURE 10: Multi-purpose drone algorithm for Union Point community

B. Delivery and Energy Efficiency Assessment

So far, we have shown that the proposed algorithm provides uniform coverage over the neighborhood area. Now we want to show that this algorithm also provides efficient delivery of packages. To do so, we measured the average delivery time of 1000 packages through simulation and showed the transport efficiency in Table II. As can be seen, our proposed algorithm delivers the packages over both communities efficiently. In Union Point, the efficiency slightly decreases because there are some cells without buildings. In general, the transport efficiency of the proposed method depends on how dense the trajectories are in the area in the first place. If we have an area, where the trajectories already cover most of the region, the efficiency is very high, e.g. in the case of UMASS campus. If the portion of uncovered area gets larger, the efficiency goes

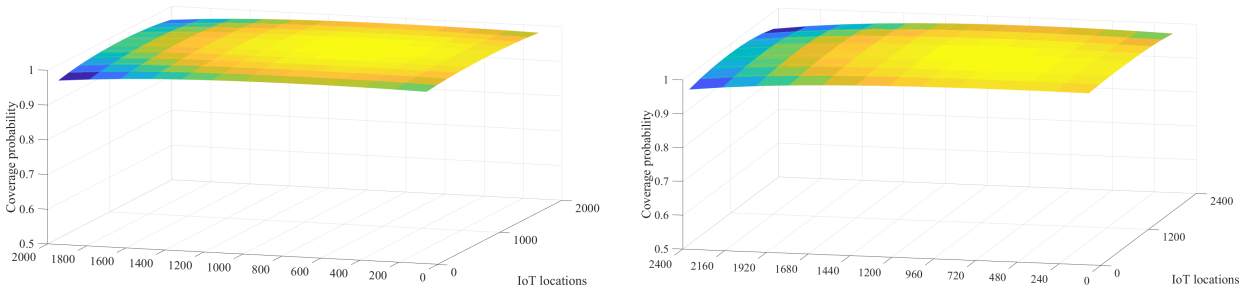

(A) UMASS campus **(B)** Union Point

FIGURE 11: int community

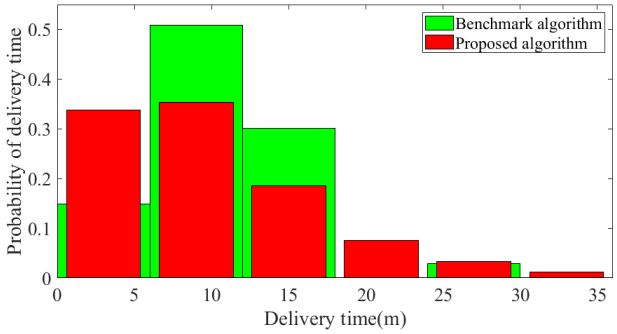

FIGURE 12: Probability of delivery time for Union Point community

down as we observed in the Union Point case.

Figure 12 shows the distribution of package delivery time for the Union Point community where the average speed is set to $V_{avg} = 20\frac{m}{s}$ for the both algorithms. As can be seen, the distribution profiles are of similar nature for the proposed algorithm and the benchmark algorithm while the latter can not provide a uniform coverage. In particular, we are interested in the fraction of packages that are delivered later than a certain amount of time, e.g., 30 minutes. This value has also been reported in Table II. As reported in this table, the fraction of these packages are very small.

Note: One may legitimately ask whether the condition of keeping the same average speed when comparing the delivery the efficiency of both algorithms is fair or not. If the drone is

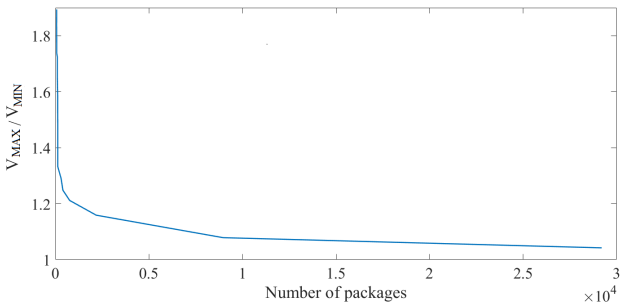

FIGURE 13: $\frac{V_{MAX}}{V_{MIN}}$ versus the number of packages that should be delivered to achieve the desired uniform coverage.

TABLE II: Average time to deliver 1000 packages with 10 drones for second algorithm

	Transport Efficiency	fraction of packages (average) with delivery time >30 mins
UMASS community	1	0.006
Union Point community	0.87	0.012

TABLE III: Propulsion energy consumption to deliver 10 packages in Union point and UMASS campus communities

	Total energy consumption(J)		Energy Efficiency
	Benchmark algorithm	Proposed algorithm	
UMASS community	1910K	1983K	0.96
Union Point community	1750K	2050K	0.85

assumed to be able to move at a speed as high as V_{MAX}, is it fair to limit the moving speed to V_{avg}? To respond to this question, we note that the proposed algorithm is quite flexible in terms of choosing the values of V_{MAX} and V_{MIN}. In fact, we can set these values such that the ratio of V_{MAX} to V_{MIN} tends to 1 (but not equal to 1) such that we have $V_{MAX} \simeq V_{MIN} \simeq V_{avg}$. The price we pay is a larger time to converge to the target coverage level. In other words, the closer this ratio is to 1, the larger number of packages have to be delivered to achieve a given level of coverage. This is while the benchmark algorithm can never provide uniform coverage. In Fig. 13, we have demonstrated this trade-off between the speed variance and the convergence time which is quantified by the number of packages that should be delivered to achieve the desired level of uniformity.

Now, we evaluate the energy performance of the proposed algorithm with respect to the benchmark algorithm which intuitively consumes less energy. We use the same energy model and parameters mentioned in [53] for both cases and define the efficiency as the ratio of energy corresponding to benchmark algorithm to that of the proposed algorithm. The results are reported in Table III where we deliver 10 packages in Union Point and UMASS campus communities. As shown in this table, the speed variation in the proposed algorithm has caused slight increase in energy consumption.

VI. Conclusion

In this paper, we proposed UAVs that simultaneously perform multiple tasks, namely uniform-coverage applications (UCAs) and transport jobs. By focusing on last-mile delivery application, we investigated the multi-task UAVs for two scenarios: i) a simplified scenario where the neighborhood area is a circular region, and ii) a practical scenario where the neighborhood area is an arbitrarily-shaped region. For each scenario, we proposed an algorithm for UCA and last-mile delivery. We proved that both algorithms provide a uniform coverage probability for a typical user within the neighborhood area. Through simulation results, we verified the uniform coverage and at the same time, we demonstrated that we can still maintain the delivery efficiency compared to the original delivery algorithm at the expense of some mild increase in the consumed energy.

References

[1] A. Barrientos, J. Colorado, J. d. Cerro, A. Martinez, C. Rossi, D. Sanz, and J. Valente, "Aerial remote sensing in agriculture: A practical approach to area coverage and path planning for fleets of mini aerial robots," *Journal of Field Robotics*, vol. 28, no. 5, pp. 667–689, Aug. 2011.

[2] L. Babel, "Curvature-constrained traveling salesman tours for aerial surveillance in scenarios with obstacles," *European Journal of Operational Research*, vol. 262, no. 1, pp. 335–346, Oct. 2017.

[3] G. Avellar, G. Pereira, L. Pimenta, and P. Iscold, "Multi-UAV routing for area coverage and remote sensing with minimum time," *Sensors*, vol. 15, no. 11, pp. 27 783–27 803, Nov. 2015.

[4] L. Lin and M. A. Goodrich, "Hierarchical heuristic search using a gaussian mixture model for UAV coverage planning," *IEEE Transactions on Cybernetics*, vol. 44, no. 12, pp. 2532–2544, Dec. 2014.

[5] A. Otto, N. Agatz, J. Campbell, B. Golden, and E. Pesch, "Optimization approaches for civil applications of unmanned aerial vehicles (UAVs) or aerial drones: A survey," *Networks*, vol. 72, no. 4, pp. 411–458, Mar. 2018.

[6] S. M. Adams and C. J. Friedland, "A survey of unmanned aerial vehicle (UAV) usage for imagery collection in disaster research and management," in *9th International Workshop on Remote Sensing for Disaster Response*, vol. 8, Jan. 2011.

[7] A. Nedjati, G. Izbirak, B. Vizvári, and J. Arkat, "Complete coverage path planning for a multi-UAV response system in post-earthquake assessment," *Robotics*, vol. 5, p. 26, Dec. 2016.

[8] M. Raap, M. Zsifkovits, and S. Pickl, "Trajectory optimization under kinematical constraints for moving target search," *Computers and Operations Research*, vol. 88, pp. 324–331, Dec. 2017.

[9] G. Zhu and P. Wei, "Pre-departure planning for urban air mobility flights with dynamic airspace reservation," in *AIAA Aviation 2019 Forum*, 2019, p. 3519.

[10] J. E. Scott and C. H. Scott, "Drone delivery models for healthcare," in *50th Hawaii International Conference on System Sciences (HICSC)*, 2017.

[11] C. C. Murray and A. G. Chu, "The flying sidekick traveling salesman problem: Optimization of drone-assisted parcel delivery," *Transportation Research Part C: Emerging Technologies*, vol. 54, pp. 86–109, 2015.

[12] N. A. H. Agatz, P. Bouman, and M. Schmidt, "Optimization approaches for the traveling salesman problem with drone," *Transportation Science*, vol. 52, no. 4, pp. 965–981, Aug. 2018.

[13] X. Wang, S. Poikonen, and B. L. Golden, "The vehicle routing problem with drones: several worst-case results," *Optimization Letters*, vol. 11, pp. 679–697, Apr. 2017.

[14] P. Tatham, F. Stadler, A. Murray, and R. Z. Shaban, "Flying maggots: a smart logistic solution to an enduring medical challenge," *Journal of Humanitarian Logistics and Supply Chain Management*, vol. 7, no. 2, pp. 172–193, Aug. 2017.

[15] A. Nedjati, B. Vizvari, and G. Izbirak, "Post-earthquake response by small UAV helicopters," *Natural Hazards*, vol. 80, no. 3, pp. 1669–1688, Feb. 2016.

[16] S. Poikonen, X. Wang, and B. Golden, "The vehicle routing problem with drones: Extended models and connections," *Networks*, vol. 70, no. 1, pp. 34–43, Aug. 2017.

[17] B. Rabta, C. Wankmüller, and G. Reiner, "A drone fleet model for last-mile distribution in disaster relief operations," *International Journal of Disaster Risk Reduction*, vol. 28, pp. 107–112, Jun. 2018.

[18] S. Chowdhury, A. Emelogu, M. Marufuzzaman, S. G. Nurre, and L. Bian, "Drones for disaster response and relief operations: A continuous approximation model," *International Journal of Production Economics*, vol. 188, pp. 167–184, Jun. 2017.

[19] R. D'Andrea, "Guest editorial can drones deliver?" *IEEE Transactions on Automation Science and Engineering*, vol. 11, pp. 647–648, Jul. 2014.

[20] A. Welch, "A cost-benefit analysis of amazon prime air," 2015.

[21] M. W. Ulmer and B. W. Thomas, "Same-day delivery with heterogeneous fleets of drones and vehicles," *Networks*, vol. 72, no. 4, pp. 475–505, Oct. 2018.

[22] Q. M. Ha, Y. Deville, Q. D. Pham, and M. H. Hà, "On the min-cost traveling salesman problem with drone," *Transportation Research Part C: Emerging Technologies*, vol. 86, pp. 597–621, Jan. 2018.

[23] N. H. Motlagh, T. Taleb, and O. Arouk, "Low-altitude unmanned aerial vehicles-based internet of things services: Comprehensive survey and future perspectives," *IEEE Internet of Things Journal*, vol. 3, no. 6, pp. 899–922, Dec. 2016.

[24] F. Ono, H. Ochiai, and R. Miura, "A wireless relay network based on unmanned aircraft system with rate optimization," *IEEE Transactions on Wireless Communications*, vol. 15, no. 11, pp. 7699–7708, Nov. 2016.

[25] M. Mozaffari, W. Saad, M. Bennis, and M. Debbah, "Unmanned aerial vehicle with underlaid device-to-device communications: Performance and tradeoffs," *IEEE Transactions on Wireless Communications*, vol. 15, no. 6, pp. 3949–3963, Jun. 2016.

[26] J. Lyu, Y. Zeng, and R. Zhang, "Cyclical multiple access in UAV-aided communications: A throughput-delay tradeoff," *IEEE Wireless Communications Letters*, vol. 5, no. 6, pp. 600–603, Dec. 2016.

[27] V. V. Chetlur and H. S. Dhillon, "Downlink coverage analysis for a finite 3-D wireless network of unmanned aerial vehicles," *IEEE Transactions on Communications*, vol. 65, no. 10, pp. 4543–4558, Oct. 2017.

[28] Y. Zeng, R. Zhang, and T. J. Lim, "Throughput maximization for UAV-enabled mobile relaying systems," *IEEE Transactions on Communications*, vol. 64, no. 12, pp. 4983–4996, Dec. 2016.

[29] Y. Sun, Z. Ding, and X. Dai, "A cooperative scheme for unmanned aerial vehicles in malfunction areas," in *Proc. IEEE 89th Vehicular Technology Conference (VTC2019-Spring)*, 2019, pp. 1–5.

[30] M. Mozaffari, W. Saad, M. Bennis, and M. Debbah, "Drone small cells in the clouds: Design, deployment and performance analysis," in *Proc. IEEE Global Communications Conference (GLOBECOM)*, 2015, pp. 1–6.

[31] J. Lyu, Y. Zeng, R. Zhang, and T. J. Lim, "Placement optimization of UAV-mounted mobile base stations," *IEEE Communications Letters*, vol. 21, no. 3, pp. 604–607, Mar. 2017.

[32] E. Kalantari, H. Yanikomeroglu, and A. Yongacoglu, "On the number and 3D placement of drone base stations in wireless cellular networks," in *Proc. IEEE 84th Vehicular Technology Conference (VTC-Fall)*, 2016, pp. 1–6.

[33] M. Mozaffari, W. Saad, M. Bennis, and M. Debbah, "Efficient deployment of multiple unmanned aerial vehicles for optimal wireless coverage," *IEEE Communications Letters*, vol. 20, no. 8, pp. 1647–1650, Aug. 2016.

[34] ——, "Mobile unmanned aerial vehicles (UAVs) for energy-efficient internet of things communications," *IEEE Transactions on Wireless Communications*, vol. 16, no. 11, pp. 7574–7589, Nov. 2017.

[35] Q. Wu, Y. Zeng, and R. Zhang, "Joint trajectory and communication design for UAV-enabled multiple access," in *Proc. IEEE Global Communications Conference (GLOBECOM)*, 2017, pp. 1–6.

[36] J. Lyu, Y. Zeng, and R. Zhang, "UAV-aided offloading for cellular hotspot," *IEEE Transactions on Wireless Communications*, vol. 17, no. 6, pp. 3988–4001, Jun. 2018.

[37] Q. Wu, Y. Zeng, and R. Zhang, "Joint trajectory and communication design for multi-UAV enabled wireless networks," *IEEE Transactions on Wireless Communications*, vol. 17, no. 3, pp. 2109–2121, Mar. 2018.

[38] C. Zhang and W. Zhang, "Spectrum sharing for drone networks," *IEEE Journal on Selected Areas in Communications*, vol. 35, no. 1, pp. 1279–1304, Jan. 2017.

[39] S. Enayati, H. Saeedi, H. Pishro-Nik, and H. Yanikomeroglu, "Moving aerial base station networks: stochastic geometry analysis and design perspective," *IEEE Transactions on Wireless Communications*, vol. 18, no. 6, pp. 2977–2988, Jun. 2019.

[40] V. Sharma, M. Bennis, and R. Kumar, "UAV-assisted heterogeneous networks for capacity enhancement," *IEEE Communications Letters*, vol. 20, no. 6, pp. 1207–1210, Jun. 2016.

[41] L. Liu, S. Zhang, and R. Zhang, "Comp in the sky: UAV placement and movement optimization for multi-user communications," *IEEE Transactions on Communications*, vol. 67, no. 8, Aug. 2019.

[42] I. Bor-Yaliniz, A. El-Keyi, and H. Yanikomeroglu, "Spatial configuration of agile wireless networks with drone-BSs and user-in-the-loop," *IEEE Transactions on Wireless Communications*, vol. 18, no. 2, pp. 753–768, Feb. 2019.

[43] Y. Zeng, Q. Wu, and R. Zhang, "Accessing from the sky: A tutorial on uav communications for 5g and beyond," *Proceedings of the IEEE*, vol. 107, no. 12, pp. 2327–2375, 2019.

[44] S. Chandrasekharan, K. Gomez, A. Al-Hourani, S. Kandeepan, T. Rasheed, L. Goratti, L. Reynaud, D. Grace, I. Bucaille,

T. Wirth *et al.*, "Designing and implementing future aerial communication networks," *IEEE Communications Magazine*, vol. 54, no. 5, pp. 26–34, May f2016.

[45] D. Ebrahimi, S. Sharafeddine, P. Ho, and C. Assi, "UAV-aided projection-based compressive data gathering in wireless sensor networks," *IEEE Internet of Things Journal*, vol. 6, no. 2, pp. 1893–1905, Apr. 2019.

[46] M. Samir, S. Sharafeddine, C. M. Assi, T. M. Nguyen, and A. Ghrayeb, "UAV trajectory planning for data collection from time-constrained IoT devices," *IEEE Transactions on Wireless Communications*, vol. 19, no. 1, pp. 34–46, Jan. 2020.

[47] J. Xu, Y. Zeng, and R. Zhang, "UAV-enabled multiuser wireless power transfer: Trajectory design and energy optimization," in *2017 23rd Asia-Pacific Conference on Communications (APCC)*, Dec. 2017, pp. 1–6.

[48] ——, "UAV-enabled wireless power transfer: Trajectory design and energy optimization," *IEEE Transactions on Wireless Communications*, vol. 17, no. 8, pp. 5092–5106, Aug. 2018.

[49] F. Huang, J. Chen, H. Wang, G. Ding, Z. Xue, Y. Yang, and F. Song, "UAV-assisted SWIPT in internet of things with power splitting: Trajectory design and power allocation," *IEEE Access*, vol. 7, pp. 68 260–68 270, May 2019.

[50] M. Bonetto, P. Korshunov, G. Ramponi, and T. Ebrahimi, "Privacy in mini-drone based video surveillance," in *Proc. 11th IEEE International Conference and Workshops on Automatic Face and Gesture Recognition (FG)*, vol. 4, 2015, pp. 1–6.

[51] J. Xiang, Y. Liu, and Z. Luo, "Flight safety measurements of uavs in congested airspace," *Chinese Journal of Aeronautics*, vol. 29, no. 5, pp. 1355–1366, 2016.

[52] M. Haenggi, *Stochastic Geometry for Wireless Networks*. Cambridge University Press, 2012.

[53] Y. Zeng, J. Xu, and R. Zhang, "Energy minimization for wireless communication with rotary-wing uav," *IEEE Transactions on Wireless Communications*, vol. 18, no. 4, pp. 2329–2345, Apr. 2019.

[54] U. Point. (2017) Union point. [Online]. Available: https://www.bldup.com/posts/1-550-acres-of-smart-sustainable-development-taking-shape-at-union-point-just-12-miles-south-of-boston